Neurological Injury and Cerebral Blood Flow in Single Ventricles Throughout Staged Surgical Reconstruction

BACKGROUND: Patients with a single ventricle experience a high rate of brain injury and adverse neurodevelopmental outcome; however, the incidence of brain abnormalities throughout surgical reconstruction and their relationship with cerebral blood flow, oxygen delivery, and carbon dioxide reactivity remain unknown.

METHODS: Patients with a single ventricle were studied with magnetic resonance imaging scans immediately prior to bidirectional Glenn (pre-BDG), before Fontan (BDG), and then 3 to 9 months after Fontan reconstruction.

RESULTS: One hundred sixty-eight consecutive subjects recruited into the project underwent 235 scans: 63 pre-BDG (mean age, 4.8±1.7 months), 118 BDG (2.9±1.4 years), and 54 after Fontan (2.4±1.0 years). Nonacute ischemic white matter changes on T2-weighted imaging, focal tissue loss, and ventriculomegaly were all more commonly detected in BDG and Fontan compared with pre-BDG patients ($P<0.05$). BDG patients had significantly higher cerebral blood flow than did Fontan patients. The odds of discovering brain injury with adjustment for surgical stage as well as ≥2 coexisting lesions within a patient decreased (63%–75% and 44%, respectively) with increasing amount of cerebral blood flow ($P<0.05$). In general, there was no association of oxygen delivery (except for ventriculomegaly in the BDG group) or carbon dioxide reactivity with neurological injury.

CONCLUSIONS: Significant brain abnormalities are commonly present in patients with a single ventricle, and detection of these lesions increases as children progress through staged surgical reconstruction, with multiple coexisting lesions more common earlier than later. In addition, this study demonstrated that BDG patients had greater cerebral blood flow than did Fontan patients and that an inverse association exists of various indexes of cerebral blood flow with these brain lesions. However, CO_2 reactivity and oxygen delivery (with 1 exception) were not associated with brain lesion development.

CLINICAL TRIAL REGISTRATION: URL: http://www.clinicaltrials.gov. Unique identifier: NCT02135081.

Mark A. Fogel, MD
Christine Li, BS
Okan U. Elci, PhD
Tom Pawlowski, BS
Peter J. Schwab, BS
Felice Wilson, RN, BSN
Susan C. Nicolson, MD
Lisa M. Montenegro, MD
Laura Diaz, MD
Thomas L. Spray, MD
J. William Gaynor, MD
Stephanie Fuller, MD
Christopher Mascio, MD
Marc S. Keller, MD
Matthew A. Harris, MD
Kevin K. Whitehead, MD
Jim Bethel, PhD
Arastoo Vossough, MD
Daniel J. Licht, MD

Correspondence to: Mark A. Fogel, MD, The Children's Hospital of Philadelphia, Division of Cardiology, 34th Street and Civic Center Boulevard, Philadelphia, PA 19104. E-mail fogel@email.chop.edu

Sources of Funding, see page 681

Key Words: cerebral infarction ■ cerebrovascular circulation ■ Fontan procedure ■ heart ventricles ■ magnetic resonance imaging

Clinical Perspective

What Is New?

- Significant brain abnormalities are commonly present in patients with a single ventricle, with detection of these lesions increasing as children progress through staged surgical reconstruction.
- An inverse association exists of various indexes of cerebral blood flow with these brain lesions.

What Are the Clinical Implications?

- Cerebral blood flow and neurological injury are potentially modifiable factors that may affect neurodevelopmental outcomes and quality of life.
- Measurement of cerebral blood flow and identification of brain abnormalities may enhance recognition of patients with a single ventricle at risk for poor outcome and facilitate early intervention if appropriate.

Besides a high risk of mortality and adverse outcomes,[1] patients with a single ventricle undergoing staged surgical reconstruction culminating in the Fontan operation face a well-known concern for poor neurological outcome resulting from both brain injury and delayed maturation.[2–7] This has presumably led to the findings of poor neurodevelopmental outcome in this patient population.[8–11] The etiology of these brain lesions is multifactorial, including genetics, cyanosis, and numerous surgeries that involve cardiopulmonary bypass and deep hypothermic circulatory arrest. In addition, the multiple surgeries that these children undergo change their physiology, pulmonary and systemic blood flow patterns, and hemodynamics over the course of their vulnerable first years of life, which may also contribute to the genesis of this issue.

The purpose of this study was to determine the prevalence of brain abnormalities in patients with a single ventricle as they progress through staged surgical reconstruction and if a link exists between cerebral blood flow (CBF) and oxygen delivery (O_2D) and cerebral abnormalities. Patients were assessed by cardiac magnetic resonance (CMR) and brain magnetic resonance imaging (MRI) immediately prior to hemi-Fontan or bidirectional Glenn (pre-BDG), immediately prior to Fontan (BDG), and 3 to 9 months after Fontan. We speculated that the CBF, O_2D, and CO_2 reactivity (ie, hypercarbia increases CBF) at various stages would correlate with brain abnormalities. The importance of these findings is not only to determine the cause of such lesions but also may lead to important changes in the approach to surgical and medical management of these patients to preserve maximal neurological function.

METHODS

Patients

This was a single-center, National Institutes of Health–sponsored, prospective study of patients with a single ventricle throughout staged surgical reconstruction; all were enrolled from April 2009 to June 2014. We included any patient <10 years of age with single-ventricle physiology undergoing elective cardiac reconstructive surgery at our institution. The patient needed to be stable enough to undergo an ≈1-hour CMR and MRI scan under general anesthesia. Exclusion criteria included contraindication to CMR and MRI (eg, pacemakers or any contraindicated ferromagnetic material). Demographics obtained included age, sex, body surface area (BSA), diagnosis, and stage of surgical reconstruction. Informed consent for participation was obtained from all participants' families. The hospital's Institutional Review Board approved the prospective study, and all patients gave informed consent.

Study Procedure

Patients underwent a CMR and MRI immediately prior to heart surgery for pre-BDG and BDG and 3 to 9 months after Fontan completion. In those prior to surgery, the patient was prepared in the operating room with intravenous and arterial line placement; all participants were administered general anesthesia of nitrous oxide and sevoflurane of ≤1 minimum alveolar concentration, paralyzed, endotracheally or nasotracheally intubated, and mechanically ventilated with a minute ventilation to achieve a $Paco_2$ of 40±2 mm Hg. The patient was then transported via stretcher to the adjacent scanner (Siemens Avanto 1.5-T whole-body MRI system, Siemens Medical Solutions, Malvern, PA). The patient was placed in the supine position, head first, into the scanner that utilized the 6-channel head coil and 8-channel body array coil; all imaging was performed at isocenter. Baseline CBF and CMR imaging was performed before 3% to 7% CO_2 was instilled into the inhaled gas to create hypercarbic conditions, increasing CBF. This lasted 15 to 20 minutes, during which time cerebral anatomy imaging was performed. At the end of the 20 minutes of hypercarbia, measurement of flows was repeated. Hypercarbic conditions aimed for a $Paco_2$ of 60 to 69 mm Hg on arterial blood gas. In those who were 3 to 9 months after Fontan, only room air conditions were studied because an arterial line was not present to measure arterial blood gases. Studies lasted ≈1 hour; afterward, the patient was immediately removed from the scan room and transported either to the operative suite where surgery was performed or to the recovery area. On completion of the MRI, the study was read by a staff neuroradiologist, and a determination was made in discussions with the neurologist and surgeon to proceed to surgery or to wake the child.[12]

CMR and MRI Protocol

To measure CBF and O_2D, 2 methodologies were used: phase-contrast magnetic resonance (PCMR) and arterial spin labeling (ASL).

1. PCMR: After localizers, a stack of static steady-state free-precession images of the thorax were obtained to assess cardiovascular anatomy and to obtain the exact slice positions and orientations for retrospective,

Circulation. 2017;135:671–682. DOI: 10.1161/CIRCULATIONAHA.116.021724

ECG-gated, through-plane PCMR that was performed across the right and left jugular veins, superior vena cava, and aorta or neoaorta. Velocity encodings across the veins were initially performed at 60 cm/s and across the aorta at 150 cm/s; if blood velocities exceeded that, a higher velocity encoding was then used. Multiple excitations were used to offset respiratory motion. The sum of the jugular veins was considered CBF, and O_2D was calculated from CBF and arterial blood gas with the following equation: $O_2D=CBF\times([0.003\times Po_2]+[1.34\times O_2sat\times Hgb])$, where Po_2 is partial pressure of oxygen (mm Hg), O_2sat is the oxygen saturation (%), and Hgb is the hemoglobin content (g/dL).

2. ASL: This perfusion technique uses magnetically labeled arterial blood water as a nominally diffusible flow tracer. The pseudocontinuous (pCASL) sequence is a modified version of the flow-sensitive alternating inversion recovery technique.[13,14] For optimal labeling, a hyperbolic secant inversion pulse is generated with MATPULSE software[15] with 15.36-millisecond duration, 17-uT radiofrequency amplitude, and 95% tagging efficiency. A gradient of 0.7 mT/m is applied along with the hyperbolic secant pulse during tag, while the hyperbolic secant pulse is applied in the absence of gradient during control. The slab of the slice-selective inversion is 10 cm thick. The saturation pulse is applied to a 10-cm slab adjacent and inferior to the selective inversion slab. A delay time (msec) is inserted between the saturation and excitation pulses. Imaging parameters were as follows: matrix size=64×64, repetition time/echo time (TR/TE)=3000/29 milliseconds, and slice thickness=8 mm with a 2-mm gap. Seven slices were be acquired sequentially from inferior to superior with a gradient echo planar imaging sequence, and each slice acquisition took about 80 milliseconds. The field of view was 20 to 22 cm.

To assess cerebral anatomy, gradient localizers were used to locate the brain and were used as a basis to perform the following anatomic brain imaging:

(1) 3-dimensional volumetric T1-weighted magnetization-prepared rapid-acquisition gradient echo (TR/TE/inversion time=1980/2.65/1100 milliseconds, flip angle=15°, slice thickness=1.5 mm, matrix=256×256);

2) 3-dimensional volumetric T2-weighted sampling perfection with application-optimized contrasts using different flip angle evolution (TR/TE=3200/453 milliseconds, slice thickness=2 mm, matrix=256×254);

(3) 3-dimensional susceptibility-weighted imaging (SWI; TR/TE=49/40 milliseconds, slice thickness=2 mm, matrix=256×177);

(4) diffusion-weighted imaging (TR/TE=2903/86 milliseconds; slice thickness=4 mm; b values=0, 500, and 100 mm/s^2; matrix 128×128); and

(5) 2-dimensional T2-weighted coronal imaging (TR/TE=6000/112 milliseconds, slice thickness=4 mm, no gap, matrix=448×336).

All images in native form and multiplanar reformat were reviewed by a pediatric neuroradiologist (A.V.) who was blinded to the results of CBF and O_2D. Abnormalities identified included nonacute ischemic changes on T2-weighted imaging, periventricular leukomalacia (PVL), focal tissue loss and atrophy (indicating subacute and chronic stroke), ventriculomegaly, and last, SWI evaluation of cerebral venous prominence (owing to high deoxyhemoglobin levels), choroid plexus susceptibility (owing to bleeds or high deoxyhemoglobin levels), and cerebral parenchymal microbleeds. Definitions of these abnormalities are given in Table 1.

Statistics

Descriptive statistics were used and recorded as mean±SD. CBF measured with PCMR was indexed to BSA and to aortic flow and brain volume (as a percent). Predictors of brain lesions included CBF, CBF/brain volume (grams), O_2D, O_2D/brain volume, and CBF_{ASL} (mL O_2/100 g brain tissue per minute). CBF reactivity was calculated by dividing the difference between CBF in room air and CBF in hypercarbia by the difference in Pco_2 between the 2 conditions; the same was done for O_2D. Logistic or ordinal regression models within each surgery stage (pre-BDG, BDG, and Fontan) separately were used as an exploratory analysis for the relationships of CBF, O_2D, CBF measured with PCMR indexed to BSA, and CBF_{ASL} with brain abnormalities. Because multiple tests were performed, we used a value of P=0.003 as a threshold for the results from these models. Mixed-effects linear regression models with random intercepts were applied to examine the change in CBF outcomes across the 3 surgery stages. Logistic regression models using generalized estimating equations were used to compare stages of surgery and to assess the relationships of CBF, O_2D, CBF measured with PCMR indexed to BSA, and CBF_{ASL} with brain abnormalities after adjustment for stage of surgery. Random intercept Poisson regression models were used for count data. A value of $P\leq 0.05$ was considered significant. Mixed-effects linear regression models with random intercepts, logistic regression models using generalized estimating equations, and Poisson regression models account for correlations arising from the repeated measures. Stata 14.2 (StataCorp, College Station, TX) software was used to conduct statistical analyses. We applied the Benjamini and Hochberg[16] false discovery rate method to derive corrected P values to address the issue of multiple testing. We used the Bonferroni procedure for the post hoc comparisons among 3 groups for CBF.

RESULTS

Study Population

One hundred sixty-eight patients with a single ventricle who underwent 235 MRI scans make up the study population; 60 subjects underwent 127 scans at different surgical stages. Figure 1 is a flow diagram of the distribution of scans at each stage and shows how many subjects had multiple scans; demographics of the patients at each stage are listed in Table 2.

Brain Lesions and Stage of Surgical Reconstruction

Stage of surgical reconstruction had a significant effect on the types of lesions observed. Table 3 lists all the brain

Table 1. Definitions of Brain Abnormalities

Brain Abnormality*	Definition
Acute ischemic changes	Any acute ischemia and infarct seen in the brain on the basis of diffusion-weighted imaging trace maps and apparent diffusion coefficient maps
Periventricular leukomalacia	Lesions with typical appearance and location of periventricular leukomalacia, including punctate white matter injury
Nonacute ischemic T2 changes	Focal lesions without acute ischemic findings that are likely to be the result of prior ischemia on the basis of imaging appearance and that follow vascular territories
Delayed myelination	Assessment of myelination based on well-established norms of myelination progression on the basis of T1- and T2-weighted images
Developmental defect (malformation)	Any congenital malformation of the brain
Generalized atrophy	Diffuse volume loss in the brain
Focal tissue loss and atrophy	Any nondiffuse focal loss and atrophy of brain parenchymal tissue
Ventriculomegaly	Enlargement of the ventricles as a result of any cause; may or may not be associated with generalized volume loss
Intracranial hemorrhage, gross (acute or chronic)	Detection of gross brain parenchymal or extra-axial hemorrhage, acute or chronic, on the basis of any combination of imaging sequences
Intraventricular hemorrhage	Presence of any new or old intraventricular hemorrhage
Operculum	Whether the sylvian operculum remains widely open or has normally closed
Susceptibility-weighted imaging veins	Presence or absence of abnormal prominence of the cortical and medullary veins on the basis of susceptibility-weighted imaging maximum-intensity projection images
Choroid plexus susceptibility	Presence or absence of susceptibility in either choroid plexus on susceptibility-weighted imaging

*Note that although these classifiers are distinct, there may often be overlap in some of the features for a particular lesion or patient.

lesions present as raw data on the MRI scans of the entire cohort, and Table 4 lists the significant differences noted by surgical stage (statistically nonsignificant differences not shown). PVL was more common in BDG than either pre-BDG or Fontans. SWI venous prominence was more common in pre-BDG than in BDG or Fontan (prominent versus normal or prominent versus borderline); these were more common in BDG than Fontan for borderline versus normal and prominent versus normal. Table 5 lists what was felt to be the 3 most important brain lesions grouped for biological plausibility (atrophy=generalized atrophy+focal tissue loss and atrophy, developmental malformations=developmental defects+delayed myelination, and hemorrhage=interventricular hemorrhage+gross intracranial hemorrhage; acute ischemic changes and PVL, also thought to be important, are listed in Table 4).

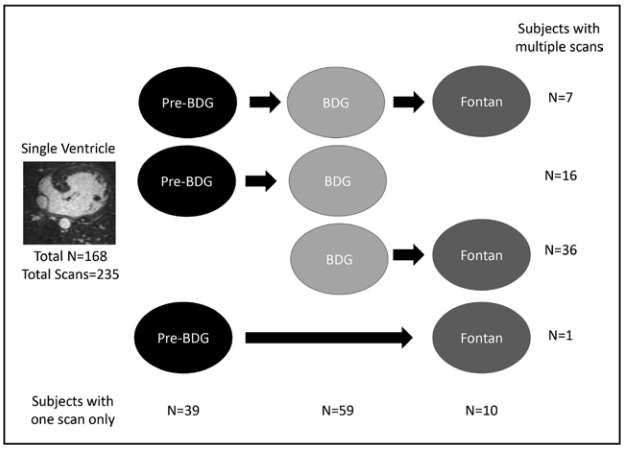

Figure 1. Breakdown of patients with single ventricle studied by stage of surgery.
Numbers on the **right** represent the number of patients with multiple scans; those at the **bottom** represent those with a single scan only. BDG indicates bidirectional Glenn.

Because multiple brain abnormalities may coexist in the same patient, the entire cohort was divided into those with ≥2 brain lesions and those with fewer. Stage of surgery had a significant effect on the number of brain abnormalities (P=0.0001). Pre-BDG and BDG had more patients with ≥2 lesions (n=59 [97%] and n=102 [90%], respectively) than the Fontan group (n=37, 70%), with odds ratios of 13.6 and 4.1, respectively (P=0.01 and 0.0005, respectively). Table 6 lists the number of brain abnormalities according to surgical stage for those who underwent multiple scans. Pre-BDG had 45% and BDG had 29% more brain abnormalities than those after Fontan (P=0.01 and 0.03 respectively).

Examples of brain lesions observed are given in Figures 2 through 5.

Association of Brain Lesions With CBF

For the entire group, CBF indexed to aortic flow, brain volume, and CBF_{ASL} was not associated with brain le-

Table 2. Demographics of Patients at Each Imaging Instance

	Pre-BDG (n=63)	BDG (n=118)	Fontan (n=54)	Total (n=235)
Male, n (%)	40 (64)	70 (60)	37 (69)	147 (64)
Female, n (%)	23 (37)	48 (41)	17 (32)	88 (37)
Age (range), y*	0.45±0.13 (0.27–0.78)	3.25±0.96 (2.08–7.64)	3.92±1.22 (2.13–8.36)	2.64±1.63 (0.27–8.36)
Height, cm*	63.2±6.20	91.7±14.04	97.3±11.79	85.7±17.93
Weight, kg*	6.30±1.12	13.4±2.96	15.7±3.02	12.1±4.41
Body surface area, m^2*	0.33±0.04	0.58±0.10	0.64±0.09	0.53±0.15
Time from prior surgery to magnetic resonance imaging, mo*	4.9±1.5	29±14.6	8.6±5.3	18.1±15.7
Heart rate, bpm†	136±25	116±20	115±20	121±23
Systolic blood pressure, mm Hg‡	107±26	110±23	99±16	107±23
Diastolic blood pressure, mm Hg§	54±16	64±20	53±17	59±19
Hemoglobin, mg/dL	13.5±1.72	15.5±1.83	N/A	14.8±2.02
Po_2 in room air/Po_2 in hypercarbia	45.8±4.05/51.5±6.13	51.7±7.19/60.3±8.94	N/A	…
O_2 saturation in room air/O_2 saturation in hypercarbia	79.6±4.77/ 76.5±7.32	83.9±6.73/83.1±6.24	N/A	…
Cardiopulmonary bypass time, min	84.6±27.39	61.1±27.77	70.0±18.21	68.5±27.20
Circulatory arrest time, min	43.1±14.69	28.0±18.66	26.5±9.81	31.3±16.89
Morphology				
Hypoplastic left heart syndrome	40	62	28	130
Tricuspid atresia	7	8	3	18
Double-outlet right ventricle	6	12	6	24
Pulmonary atresia	4	11	8	23
Unbalanced atrioventricular canal	3	13	4	20
Transposition of the great arteries	0	4	0	4
Double-inlet left ventricle	0	4	4	8
Other	3	4	1	8

BDG indicates bidirectional Glenn.
*$P<0.05$ for comparison between all 3 groups.
†$P<0.05$ for comparison between all 3 groups except BDG versus Fontan.
‡$P<0.05$ for comparison between BDG and Fontan.
§$P<0.05$ for comparison between all 3 groups except pre-BDG versus Fontan.

sions in the pre-BDG group. In Fontan, with a 1% increase in CBF, the odds of nonacute ischemic changes on T2 decrease by 7.8% ($P=0.0003$), and the odds of prominent SWI venous prominence compared with combined normal and borderline SWI venous prominence decrease by 4.2% ($P=0.0025$).

Results from the logistic regression analysis using generalized estimating equations for the relationships of brain abnormalities with CBF/BSA and CBF_{ASL} after adjustment for stage effect are presented in Tables 7 and 8, respectively. After correction for multiple testing, the odds of nonacute ischemic changes on T2, focal tissue loss and atrophy, and SWI veins (borderline versus normal) all decrease (by 63%, 75%, and 73%, respectively) with 1% increasing amount of CBF by PCMR. For CBF by pCASL, with a 1-unit increase, the odds of PVL and focal tissue loss and atrophy decreased (by 33% and 9%, respectively).

For those patients with serial MRI scans, Figure 6 demonstrates the change in CBF/BSA and pCASL across stages. Results from the mixed-effects linear regression models with random intercepts reveal that the BDG patients had significantly higher CBF/BSA and CBF as measured by pCASL than Fontan patients ($P=0.005$ and $P=0.01$ respectively).

In an analysis of the number of coexistent brain lesions, for the entire cohort, the odds for ≥2 brain lesions decreases by 34% with a 1-unit increase in CBF/

Table 3. Descriptive Data of Brain Abnormalities, by Surgical Stage

Brain Abnormality	Pre-BDG, n (%)	BDG, n (%)	Fontan, n (%)	Total, n (%)
Nonacute ischemic T2 changes				
No	57 (93)	70 (62)	37 (70)	164 (72)
Yes	4 (7)	43 (38)	16 (30)	63 (29)
Acute ischemic changes, diffusion-weighted imaging/apparent diffusion coefficient				
No	60 (99)	112 (99)	53 (100)	225 (99)
Yes	2 (3)	1 (1)	0 (0)	3 (1)
Periventricular leukomalacia				
No	52 (84)	65 (59)	39 (72)	156 (69)
Yes	10 (16)	46 (41)	15 (28)	71 (31)
Generalized atrophy				
No	61 (98)	102 (90)	49 (91)	212 (92)
Borderline	1 (2)	6 (5)	3 (6)	10 (4)
Yes	0 (0)	6 (5)	2 (4)	8 (4)
Focal tissue loss and atrophy				
No	58 (94)	87 (78)	44 (82)	189 (83)
Yes	4 (7)	24 (22)	10 (19)	38 (17)
Ventriculomegaly				
No	47 (76)	73 (64)	33 (62)	153 (67)
Borderline	12 (19)	22 (19)	13 (25)	47 (21)
Yes	3 (5)	19 (17)	7 (13)	29 (13)
Susceptibility-weighted imaging veins				
Normal	1 (2)	25 (22)	29 (54)	55 (24)
Borderline	5 (8)	58 (51)	17 (32)	80 (35)
Prominent	55 (90)	30 (27)	8 (15)	93 (41)
Choroid plexus susceptibility				
No	5 (8)	43 (38)	44 (81)	92 (40)
Yes	56 (92)	70 (62)	10 (19)	136 (60)
Delayed myelination				
No	60 (97)	110 (99)	53 (98)	223 (98)
Yes	2 (3)	1 (1)	1 (2)	4 (2)
Intracranial hemorrhage, gross (acute or chronic)				
No	54 (87)	107 (95)	49 (93)	210 (92)
Yes	8 (13)	6 (5)	4 (8)	18 (8)
Developmental defect (malformation)				
No	59 (95)	107 (95)	51 (94)	217 (95)
Yes	3 (5)	6 (5)	3 (6)	12 (5)
Intraventricular hemorrhage				
No	58 (97)	112 (98)	53 (98)	223 (98)
Yes	2 (3)	2 (2)	1 (2)	5 (2)
Operculum				
Closed	30 (49)	107 (95)	51 (94)	188 (83)
Open	31 (51)	6 (5)	3 (6)	40 (18)

BDG indicates bidirectional Glenn.

BSA (P=0.01), and this result stayed significant after adjustment for surgery (a decrease of 44% with a 1-unit increase in CBF/BSA; P=0.0061). For those with serial MRIs, a 1-unit increase in CBF/BSA within a subject was associated with a 20% decrease in the number of brain abnormalities after adjustment for surgery (P=0.01).

Association of Brain Lesions With O_2D

There was no significant effect of O_2D on brain abnormalities across all 3 stages of surgical reconstruction except for ventriculomegaly in the BDG stage, for which a 1-unit increase in CBF decreased the odds of definite ventriculomegaly compared with combined no and borderline ventriculomegaly by 1% (P=0.05).

Association of Brain Lesions With Reactivity

No significant effect was noted on the reactivity on the odds of observing brain abnormalities.

DISCUSSION

This study is the first to investigate brain abnormalities throughout staged surgical reconstruction in patients with a single ventricle both as a cross section and with serial imaging. Our data demonstrated that significant brain injuries are commonly present in patients with a single ventricle and that there is an accumulation of the number of patients with injury (eg, nonacute ischemic changes, atrophy, and ventriculomegaly) as the children progress to Fontan; although this may be expected, it is the first time that this has been documented. Exceptions to this generalization include PVL (more commonly seen at the BDG stage), SWI venous prominence, choroid plexus susceptibility, and open operculum, which were all more common in pre-BDG. PVL is easily detectable in the neonate and young infant, but small foci of punctate white matter PVL injury typically fade over time and hence may no longer be detectable by standard MRI. Similarly, the operculum gradually closes as the brain matures. Prominence of the cerebral veins on SWI is closely related to excessive relative level of deoxyhemoglobin in the cerebral vessels, which was shown to decrease after the pre-BDG stage. Similarly, choroid plexus susceptibility is due to relative deoxyhemoglobin levels

Circulation. 2017;135:671–682. DOI: 10.1161/CIRCULATIONAHA.116.021724

Table 4. Logistic Regression Analysis With Generalized Estimating Equations of Brain Abnormalities

End Points	Odds Ratio (95% CI)	*P* Value
Nonacute ischemic T2 changes		0.0001
BDG vs pre-BDG	8.75 (3.173–24.150)	<0.0001
Fontan vs pre-BDG	6.16 (2.007–18.916)	0.0015
Fontan vs BDG	0.70 (0.418–1.185)	0.1866
Periventricular leukomalacia		0.0002
BDG vs pre-BDG	3.68 (1.834–7.383)	0.0002
Fontan vs pre-BDG	2.00 (0.896–4.462)	0.0905
Fontan vs BDG	0.54 (0.329–0.899)	0.0175
Ventriculomegaly		
Yes vs no		0.0237
BDG vs pre-BDG	2.84 (1.342–6.028)	0.0064
Fontan vs pre-BDG	2.53 (1.205–5.319)	0.0142
Fontan vs BDG	0.89 (0.667–1.187)	0.4269
Susceptibility-weighted imaging veins		
Borderline vs normal		0.0008
BDG vs pre-BDG	0.48 (0.055–4.229)	0.5099
Fontan vs pre-BDG	0.12 (0.014–1.077)	0.0583
Fontan vs BDG	0.25 (0.119–0.543)	0.0004
Prominent vs normal		<0.0001
BDG vs pre-BDG	0.02 (0.003–0.179)	0.0004
Fontan vs pre-BDG	0.01 (0.001–0.043)	<0.0001
Fontan vs BDG	0.23 (0.096–0.557)	0.0011
Prominent vs borderline		<0.0001
BDG vs pre-BDG	0.05 (0.016–0.127)	<0.0001
Fontan vs pre-BDG	0.04 (0.011–0.142)	<0.0001
Fontan vs BDG	0.88 (0.351–2.221)	0.7911

Only significant differences are shown. BDG indicates bidirectional Glenn; and CI, confidence interval.

and small choroid plexus bleeds. This appearance also decreased after the pre-BDG stage.

A greater number of patients in the pre-BDG and BDG groups demonstrated more coexisting brain abnormalities than Fontan patients. This would be expected because brain abnormalities in this study are a function of being congenital (eg, developmental malformations, operculum), being acquired (eg, stroke), healing, and being detectable. For example, an infant may have an operculum and PVL, both of which may not be evident on magnetic resonance because of closure of the operculum and the decreasing detectability of PVL as the patient ages.

This study also demonstrated an inverse association of various indexes of CBF with these brain abnormalities (ie, the higher the CBF, the lower the incidence of abnormalities) as either a single lesion or multiple coexistent abnormalities. CO_2 reactivity and O_2D (except for ventriculomegaly in the BDG group), however, were not associated with brain lesion development. Note that there may be some overlap between the brain injury variables evaluated in this study such as between atrophy and ventriculomegaly or between nonacute ischemic T2 changes and focal tissue loss, which were accounted for in the 3 to 5 main groups we chose. However, we chose all these variables to capture a larger number of features.

Table 5. Descriptive Data of Grouped Brain Abnormalities, by Surgical Stage

Brain Abnormality	Pre-BDG, n (%)	BDG, n (%)	Fontan, n (%)	Total, n (%)
Atrophy				
No	57 (92)	82 (73)	40 (74)	179 (78)
Yes	5 (8)	31 (27)	14 (26)	50 (22)
Developmental malformations				
No	57 (92)	104 (95)	50 (93)	211 (93)
Yes	5 (8)	6 (6)	4 (7)	15 (7)
Hemorrhage				
No	51 (85)	105 (93)	48 (91)	204 (90)
Yes	9 (15)	8 (7)	5 (9)	22 (10)

BDG indicates bidirectional Glenn.

Neonates and infants with congenital heart disease undergoing magnetic resonance have been found to have significant brain lesions before and after cardiac surgery,[2,7,17–19] with the incidence increasing with brain immaturity.[20] In the case of single-ventricle lesions, reasons for preoperative neurological injury may include

Table 6. Number of Brain Lesions in Individual Patients, by Surgical Stage

Brain Abnormalities, n	Pre-BDG, n (%)	BDG, n (%)	Fontan, n (%)	Total, n (%)
0	1 (4)	4 (7)	9 (21)	14 (11)
1	0 (0)	10 (18)	11 (26)	21 (17)
2	5 (21)	15 (26)	7 (16)	27 (22)
3	9 (38)	10 (18)	6 (14)	25 (20)
4	3 (13)	6 (11)	7 (16)	16 (13)
5	3 (13)	8 (14)	1 (2)	12 (10)
6	2 (8)	2 (4)	0 (0)	4 (3)
7	1 (4)	2 (4)	2 (5)	5 (4)
Total	24	57	43	124*

BDG indicates bidirectional Glenn.
*Three uninterpretable data sets, leaving 124 instead of 127 scans.

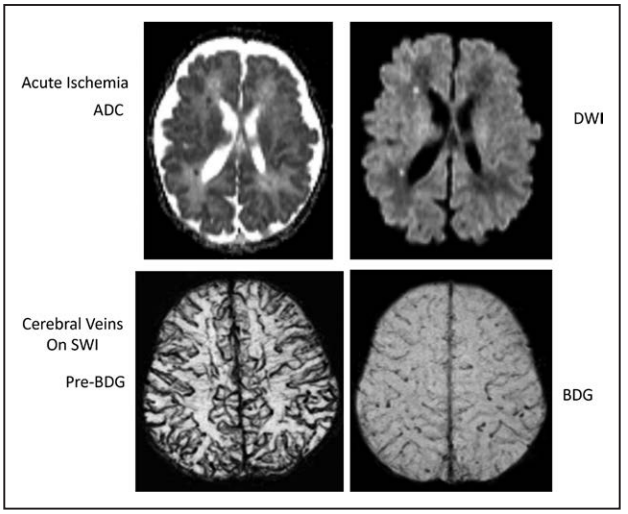

Figure 2. Example of acute ischemia on diffusion imaging and cerebral veins on susceptibility-weighted images (SWI).
ADC indicates apparent diffusion coefficient; BDG, bidirectional Glenn; and DWI, diffusion-weighted imaging.

genetic syndromes, low cardiac output, and events such as cardiac arrest, fetal and neonatal ischemia, and cyanosis causing hypoxia. Postoperatively, cardiopulmonary bypass, deep hypothermic circulatory arrest, and cerebral emboli may also contribute to the development of cerebral lesions, in addition to the preoperative causes. Although cardiopulmonary bypass and hypothermic circulatory arrest could cause expansion and progression of cerebral hemorrhage by heparinization of an already damaged brain,[21,22] there is debate in the literature as to whether these procedures do[4,18,19] or do not[23,24] put patients at risk. Our study clearly demonstrated that many neurological lesions become greater in the number of patients affected as they undergo an increased number of surgeries; whether that has to do with surgical factors alone or other factors such as the natural course of the

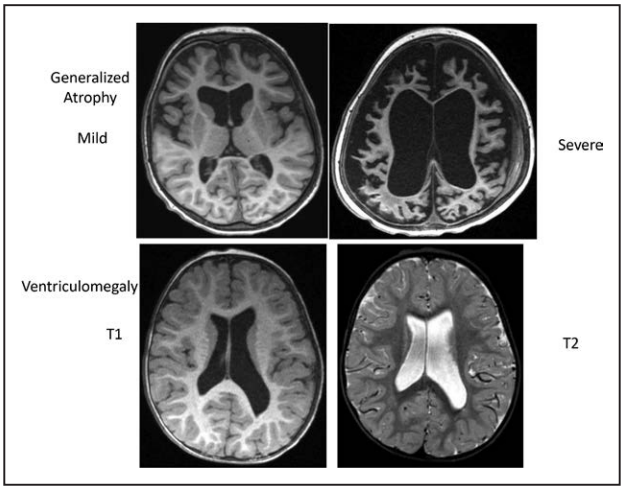

Figure 3. Example of generalized atrophy and ventriculomegaly.

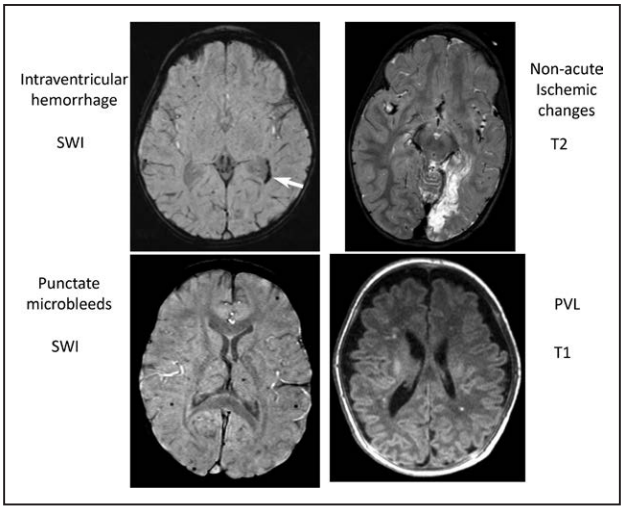

Figure 4. Example of intraventricular hemorrhage on susceptibility-weighted images (SWI), nonacute ischemic changes, punctate microbleeds on SWI, and punctate periventricular leukomalacia (PVL).

disease remains a question. It also should be noted that white matter injury is easier to visualize in the myelinated versus unmyelinated brain, which would make it more likely to be identified in the older versus the younger brain. Stroke risk increases with time in a single ventricle,[25] and chronic hypoxia may increase risk for white matter injury and loss of cortical volume.

The frequency of abnormalities consistent with focal stroke in the pre-BDG stage in our study was ≈15% (acute and nonacute ischemic changes+focal tissue loss). There are a number of reports of preoperative stroke in the literature in patients with a single ventricle undergoing neonatal surgery, ranging from the report by

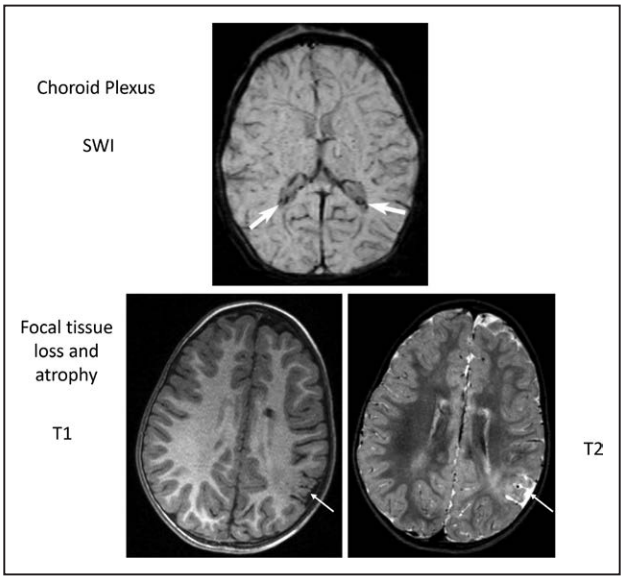

Figure 5. Example of choroid plexus susceptibility and focal tissue loss and atrophy.
SWI indicates susceptibility-weighted image.

Circulation. 2017;135:671–682. DOI: 10.1161/CIRCULATIONAHA.116.021724

Table 7. Logistic Regression Analysis With Generalized Estimating Equations of Brain Abnormalities Using Cerebral Blood Flow as Measured by Phase-Contrast Magnetic Resonance Indexed to Body Surface Area as a Covariate

End Points	Odds Ratio (95% CI)	*P* Value
Nonacute ischemic T2 changes		
Yes vs no	0.61 (0.43–0.87)	0.0061
Periventricular leukomalacia		
Yes vs no	0.88 (0.71–1.10)	0.27
Focal tissue loss and atrophy		
Yes vs no	0.50 (0.32–0.77)	0.002
Ventriculomegaly		
Borderline vs no	1.00 (0.95–1.04)	0.89
Yes vs no	0.58 (0.32–1.05)	0.0704
Yes vs borderline	0.57 (0.32–1.00)	0.0496
Susceptibility-weighted imaging veins		
Borderline vs normal	0.52 (0.34–0.79)	0.0023
Prominent vs normal	0.74 (0.51–1.09)	0.13
Prominent vs borderline	1.11 (0.73–1.69)	0.61

The odds ratio is reported for 0.5-unit (≈1 SD) increase in cerebral blood flow as measured by phase-contrast magnetic resonance indexed to body surface area. CI indicates confidence interval.

Miller et al[17] with 8% to that by Andropoulos et al[20] with 14% and Block et al[24] with 17% of patients. Our number is consistent with their studies.

The inverse association of CBF with the various neurological injuries seen in patients with a single ventricle, after adjustment for stage of surgery, although suggesting a link between these cerebral hemodynamics and anatomy, does not parse out cause and effect. Decreased CBF may be a cause of or may be caused by anatomic brain abnormalities. Other studies have found this same inverse association; for example, Licht et al[5] demonstrated the inverse link between CBF and PVL in a study of 25 term infants with congenital heart disease, whereas Fukuda et al found this in 2 studies, one with 36[26] and one with 67 low-birth-weight infants.[27] Riela et al[28] showed that regional CBF was decreased in the region of the lesions in Sturge-Weber syndrome in children. However, this has been also demonstrated in adults; for example, Doi et al[29] found that microbleeds were inversely associated with CBF in Alzheimer disease.

This study used both PCMR and pCASL to measure CBF. Each technique has its own advantages and disadvantages, including differences in accuracy, the wider availability of PCMR, and its ability to yield velocity and the anatomic and regional delineation of CBF that pCASL can acquire. In addition, pCASL generally has a lower signal-to-noise ratio than PCMR, although jugular PCMR will not account for smaller posterior cerebral draining vessels. Last, pCASL measures blood in the brain, whereas PCMR measures blood draining from the brain. All these factors may be the reason why both PCMR and pCASL correlated with focal tissue loss and atrophy, but PCMR correlated with SWI veins and nonacute ischemic changes (pCASL did not), and pCASL correlated with PVL (PCMR did not).

There was no association detected between O_2D and CO_2 reactivity with cerebral injury with 1 exception. Because O_2D was a global measurement, the lesions found may not have affected or be caused by a global measurement as opposed to a regional measurement. As for CO_2 reactivity, injury may either increase or decrease CBF or be variable because of loss of regulatory centers. If it is random or based on other physiological factors such as total cardiac index or amount of aortic to pulmonary collateral flow,[30] then it is no surprise that there is no systematic correlation either way. Similarly, CO_2 reactivity was a global measurement, and the same reasoning may apply. It is true that CBF was also a global measurement; however, the total amount of blood flow appears to be more important than O_2D.

One significance of this study is that various lesions on brain MRIs in children[31–34] and decreased CBF[35–40] have been correlated with adverse neurodevelopmental outcome. The mechanism for neurological injury alone

Table 8. Logistic Regression Analysis With Generalized Estimating Equations of Brain Abnormalities Using Cerebral Blood Flow as Measured by Pseudocontinuous Arterial Spin Labeling as a Covariate

End Points	Odds Ratio (95% CI)	*P* Value
Nonacute ischemic T2 changes		
Yes vs no	0.90 (0.82–.99)	0.0299
Periventricular leukomalacia		
Yes vs no	0.67 (0.49–0.90)	0.0071
Focal tissue loss and atrophy		
Yes vs no	0.91 (0.84–0.97)	0.0082
Ventriculomegaly		
Borderline vs no	0.94 (0.76–1.16)	0.58
Yes vs no	0.92 (0.84–1.01)	0.0717
Yes vs borderline	0.93 (0.84–1.04)	0.19
Susceptibility-weighted imaging veins		
Borderline vs normal	1.79 (0.77–4.17)	0.18
Prominent vs normal	1.41 (0.79–2.53)	0.25
Prominent vs borderline	0.84 (0.59–1.18)	0.31

The odds ratio is reported for a 1-unit (≈1 SD) increase in cerebral blood flow as measured by pseudocontinuous arterial spin labeling. CI indicates confidence interval.

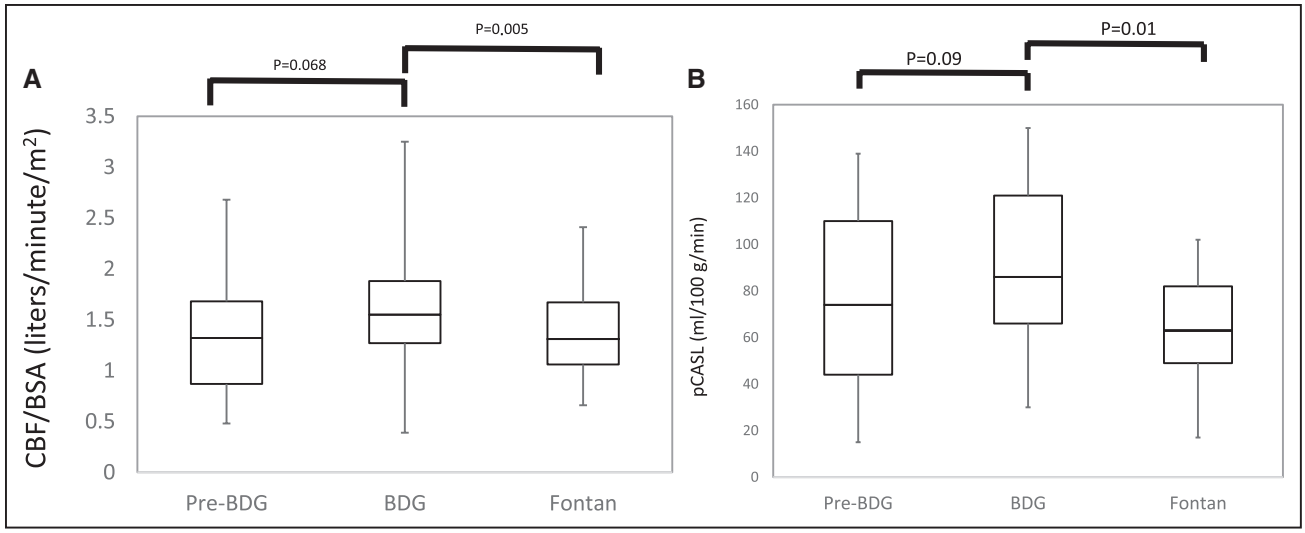

Figure 6. Plot of cerebral blood flow/body surface area (CBF/BSA; A) and pseudocontinuous arterial spin labeling (pCASL; B) in patients with serial magnetic resonance images.
There were 24, 57, and 43 scans in patients at the pre–bidirectional Glenn (pre-BDG), BDG, and Fontan stage, respectively, for a total of 124 scans in 60 patients. See Figure 1 and Table 6 for further delineation of patients with serial scans.

impairing outcome is clear. In addition, the brain requires a certain amount of CBF to function independently of neurological injury; a recent review of 25 studies bears this out.[41] In a study by Koide et al,[42] CBF and cognitive function were measured in 14 bradycardic adults before and after pacemaker implantation. Before implantation, verbal cognitive function was lower in bradycardic patients than in age-matched control subjects, but after pacemaker implantation, both CBF and verbal intelligence improved. Combining the concepts of neurodevelopment, anatomic brain lesions, and CBF with poor neurodevelopmental outcomes in patients with a single ventricle[8–11] presents a plausible mechanism for these less-than-optimal results. In our study of patients with serial MRIs, those in the BDG stage had higher CBF/BSA than Fontan patients. We speculate that techniques to improve cerebral preservation and to increase CBF (eg, increasing cardiac output) or possibly even leaving patients in the BDG stage for as long as hemodynamically possible may lead to optimizing neurological outcome. In the least, measurement of CBF and identification of brain abnormalities may enhance recognition of patients with a single ventricle at risk for poor outcome and facilitate early intervention if appropriate. Studies are currently underway to address this speculation.

Limitations

Our study cannot make a recommendation on the routine use of preoperative brain MRI or CBF throughout staged surgical reconstruction because of a lack of knowledge of whether it might contribute to poor outcomes in patients who do not receive preoperative brain MRIs, although this study suggests that this strategy may be useful and may have clinical implications. Further investigations are underway to make a definitive statement.

As previously noted, this investigation makes an association between CBF and neurological injury and does not tease out cause and effect. A longer-range study with a more complicated design would be needed to determine this.

As a result of the lack of painful stimuli, patients did not require deep levels of anesthesia, and therefore, anesthetic levels were kept as light as possible (<1 minimum alveolar concentration) while CBF was measured. This may have had an effect on CBF. However, sevoflurane, which has the least effect on CBF, was chosen as the anesthetic.

Conclusions

Significant brain abnormalities are commonly present in patients with a single ventricle, and detection of these lesions increase as children progress through staged surgical reconstruction, with multiple coexisting lesions more common earlier than later. In addition, this study has demonstrated an inverse association of various indexes of CBF with these brain lesions; however, CO_2 reactivity and O_2D (except for ventriculomegaly in the BDG group) were not associated with brain lesion development. We speculate that techniques to improve cerebral preservation and to increase CBF may lead to optimizing neurological outcome and that measuring CBF and identifying brain abnormalities may be enable the identification of patients with a single ventricle at risk for poor outcome. Studies are currently underway to address this speculation.

SOURCES OF FUNDING

This study was funded by National Heart, Lung, and Blood Institute grant 1R01HL090615-01 (principal investigator, Dr Fogel); National Institute of Neurological Disorders and Stroke 1RO1NS072338, RO1NS060653, U01HD087180 (Principal investigator: Dr Licht); and the June and Steve Wolfson Family Foundation (Principal investigator: Dr Licht).

DISCLOSURES

Dr Fogel receives grants from Edwards Life Sciences and AMAG Pharmaceuticals, Inc. The other authors report no conflicts.

AFFILIATIONS

From Division of Cardiology, Department of Pediatrics (M.A.F., C.L., T.P., F.W., M.A.H., K.K.W.), Department of Radiology (M.A.F., M.S.K., M.A.H., K.K.W., A.V.), Department of Anesthesiology and Critical Care Medicine (S.C.N., L.M.M., L.D.), Division of Cardiothoracic Surgery, Department of Surgery (T.L.S., J.W.G., S.F., C.M.), and Department of Neurology (P.J.S., D.J.L.), The Children's Hospital of Philadelphia/Perelman School of Medicine, University of Pennsylvania, Philadelphia; and Westat, Rockville, MD (O.U.E., J.B.).

FOOTNOTES

Received January 25, 2016; accepted December 12, 2016.

Circulation is available at http://circ.ahajournals.org.

REFERENCES

1. Ohye RG, Sleeper LA, Mahony L, Newburger JW, Pearson GD, Lu M, Goldberg CS, Tabbutt S, Frommelt PC, Ghanayem NS, Laussen PC, Rhodes JF, Lewis AB, Mital S, Ravishankar C, Williams IA, Dunbar-Masterson C, Atz AM, Colan S, Minich LL, Pizarro C, Kanter KR, Jaggers J, Jacobs JP, Krawczeski CD, Pike N, McCrindle BW, Virzi L, Gaynor JW; Pediatric Heart Network Investigators. Comparison of shunt types in the Norwood procedure for single-ventricle lesions. *N Engl J Med*. 2010;362:1980–1992. doi: 10.1056/NEJMoa0912461.
2. Mahle WT, Tavani F, Zimmerman RA, Nicolson SC, Galli KK, Gaynor JW, Clancy RR, Montenegro LM, Spray TL, Chiavacci RM, Wernovsky G, Kurth CD. An MRI study of neurological injury before and after congenital heart surgery. *Circulation*. 2002;106(suppl 1):I109–I114.
3. Licht DJ, Shera DM, Clancy RR, Wernovsky G, Montenegro LM, Nicolson SC, Zimmerman RA, Spray TL, Gaynor JW, Vossough A. Brain maturation is delayed in infants with complex congenital heart defects. *J Thorac Cardiovasc Surg*. 2009;137:529–536. doi: 10.1016/j.jtcvs.2008.10.025.
4. Tavani F, Zimmerman RA, Clancy RR, Licht DJ, Mahle WT. Incidental intracranial hemorrhage after uncomplicated birth: MRI before and after neonatal heart surgery. *Neuroradiology*. 2003;45:253–258. doi: 10.1007/s00234-003-0946-8.
5. Licht DJ, Wang J, Silvestre DW, Nicolson SC, Montenegro LM, Wernovsky G, Tabbutt S, Durning SM, Shera DM, Gaynor JW, Spray TL, Clancy RR, Zimmerman RA, Detre JA. Preoperative cerebral blood flow is diminished in neonates with severe congenital heart defects. *J Thorac Cardiovasc Surg*. 2004;128:841–849. doi: 10.1016/j.jtcvs.2004.07.022.
6. Galli KK, Zimmerman RA, Jarvik GP, Wernovsky G, Kuypers MK, Clancy RR, Montenegro LM, Mahle WT, Newman MF, Saunders AM, Nicolson SC, Spray TL, Gaynor JW, Galli KK. Periventricular leukomalacia is common after neonatal cardiac surgery. *J Thorac Cardiovasc Surg*. 2004;127:692–704. doi: 10.1016/j.jtcvs.2003.09.053.
7. Goff DA, Shera DM, Tang S, Lavin NA, Durning SM, Nicolson SC, Montenegro LM, Rome JJ, Gaynor JW, Spray TL, Vossough A, Licht DJ. Risk factors for preoperative periventricular leukomalacia in term neonates with hypoplastic left heart syndrome are patient related. *J Thorac Cardiovasc Surg*. 2014;147:1312–1318. doi: 10.1016/j.jtcvs.2013.06.021.
8. Ravishankar C, Zak V, Williams IA, Bellinger DC, Gaynor JW, Ghanayem NS, Krawczeski CD, Licht DJ, Mahony L, Newburger JW, Pemberton VL, Williams RV, Sananes R, Cook AL, Atz T, Khaikin S, Hsu DT; Pediatric Heart Network Investigators. Association of impaired linear growth and worse neurodevelopmental outcome in infants with single ventricle physiology: a report from the Pediatric Heart Network Infant Single Ventricle Trial. *J Pediatr*. 2013;162:250–6.e2. doi: 10.1016/j.jpeds.2012.07.048.
9. Wernovsky G, Stiles KM, Gauvreau K, Gentles TL, duPlessis AJ, Bellinger DC, Walsh AZ, Burnett J, Jonas RA, Mayer JE Jr, Newburger JW. Cognitive development after the Fontan operation. *Circulation*. 2000;102:883–889.
10. Mahle WT, Clancy RR, Moss EM, Gerdes M, Jobes DR, Wernovsky G. Neurodevelopmental outcome and lifestyle assessment in school-aged and adolescent children with hypoplastic left heart syndrome. *Pediatrics*. 2000;105:1082–1089.
11. Forbess JM, Visconti KJ, Hancock-Friesen C, Howe RC, Bellinger DC, Jonas RA. Neurodevelopmental outcome after congenital heart surgery: results from an institutional registry. *Circulation*. 2002;106(suppl 1):I95–I102.
12. Fogel MA, Pawlowski T, Schwab PJ, Nicolson SC, Montenegro LM, Berenstein LD, Spray TL, Gaynor JW, Fuller S, Keller MS, Harris MA, Whitehead KK, Vossough A, Licht DJ. Brain magnetic resonance immediately before surgery in single ventricles and surgical postponement. *Ann Thorac Surg*. 2014;98:1693–1698. doi: 10.1016/j.athoracsur.2014.05.079.
13. Kim SG. Quantification of relative cerebral blood flow change by flow-sensitive alternating inversion recovery (FAIR) technique: application to functional mapping. *Magn Reson Med*. 1995;34:293–301.
14. Wang J, Alsop DC, Li L, Listerud J, Gonzalez-At JB, Schnall MD, Detre JA. Comparison of quantitative perfusion imaging using arterial spin labeling at 1.5 and 4.0 Tesla. *Magn Reson Med*. 2002;48:242–254. doi: 10.1002/mrm.10211.
15. Matson GB. An integrated program for amplitude-modulated RF pulse generation and re-mapping with shaped gradients. *Magn Reson Imaging*. 1994;12:1205–1225.
16. Benjamini Y, Hochberg Y. Controlling the false discovery rate: a practical and powerful approach to multiple testing. *J Royal Stat Soc Series B*. 1995;57:289–300.
17. Miller SP, McQuillen PS, Hamrick S, Xu D, Glidden DV, Charlton N, Karl T, Azakie A, Ferriero DM, Barkovich AJ, Vigneron DB. Abnormal brain development in newborns with congenital heart disease. *N Engl J Med*. 2007;357:1928–1938. doi: 10.1056/NEJMoa067393.
18. Dent CL, Spaeth JP, Jones BV, Schwartz SM, Glauser TA, Hallinan B, Pearl JM, Khoury PR, Kurth CD. Brain magnetic resonance imaging abnormalities after the Norwood procedure using regional cerebral perfusion. *J Thorac Cardiovasc Surg*. 2006;131:190–197. doi: 10.1016/j.jtcvs.2005.10.003.
19. McQuillen PS, Barkovich AJ, Hamrick SE, Perez M, Ward P, Glidden DV, Azakie A, Karl T, Miller SP. Temporal and anatomic risk profile of brain injury with neonatal repair of congenital heart

defects. *Stroke*. 2007;38(suppl):736–741. doi: 10.1161/01.STR.0000247941.41234.90.
20. Andropoulos DB, Hunter JV, Nelson DP, Stayer SA, Stark AR, McKenzie ED, Heinle JS, Graves DE, Fraser CD. Brain immaturity is associated with brain injury before and after neonatal cardiac surgery with high-flow bypass and cerebral oxygenation monitoring. *J Thorac Cardiovasc Surg*. 2010;139:543–556.
21. Woodman RC, Harker LA. Bleeding complications associated with cardiopulmonary bypass. *Blood*. 1990;76:1680–1697.
22. Monagle P, Chalmers E, Chan A, DeVeber G, Kirkham F, Massicotte P, Michelson AD for the American College of Chest Physicians. Antithrombotic therapy in neonates and children: American College of Chest Physicians Evidence-Based Clinical Practice Guidelines (8th edition) *Chest*. 2008; 133(suppl):887S–968S.
23. Beca J, Gunn JK, Coleman L, Hope A, Reed PW, Hunt RW, Finucane K, Brizard C, Dance B, Shekerdemian LS. New white matter brain injury after infant heart surgery is associated with diagnostic group and the use of circulatory arrest. *Circulation*. 2013;127:971–979. doi: 10.1161/CIRCULATIONAHA.112.001089.
24. Block AJ, McQuillen PS, Chau V, Glass H, Poskitt KJ, Barkovich AJ, Esch M, Soulikias W, Azakie A, Campbell A, Miller SP. Clinically silent preoperative brain injuries do not worsen with surgery in neonates with congenital heart disease. *J Thorac Cardiovasc Surg*. 2010;140:550–557. doi: 10.1016/j.jtcvs.2010.03.035.
25. Khairy P, Fernandes SM, Mayer JE Jr, Triedman JK, Walsh EP, Lock JE, Landzberg MJ. Long-term survival, modes of death, and predictors of mortality in patients with Fontan surgery. *Circulation*. 2008;117:85–92. doi: 10.1161/CIRCULATIONAHA.107.738559.
26. Fukuda S, Mizuno K, Kakita H, Kato T, Hussein MH, Ito T, Daoud GA, Kato I, Suzuki S, Togari H. Late circulatory dysfunction and decreased cerebral blood flow volume in infants with periventricular leukomalacia. *Brain Dev*. 2008;30:589–594. doi: 10.1016/j.braindev.2008.02.001.
27. Fukuda S, Kato T, Kakita H, Yamada Y, Hussein MH, Kato I, Suzuki S, Togari H. Hemodynamics of the cerebral arteries of infants with periventricular leukomalacia. *Pediatrics*. 2006;117:1–8. doi: 10.1542/peds.2004-1719.
28. Riela AR, Stump DA, Roach ES, McLean WT Jr, Garcia JC. Regional cerebral blood flow characteristics of the Sturge-Weber syndrome. *Pediatr Neurol*. 1985;1:85–90.
29. Doi H, Inamizu S, Saito BY, Murai H, Araki T, Kira J. Analysis of cerebral lobar microbleeds and a decreased cerebral blood flow in a memory clinic setting. *Intern Med*. 2015;54:1027–1033. doi: 10.2169/internalmedicine.54.3747.
30. Fogel MA, Li C, Wilson F, Pawlowski T, Nicolson SC, Montenegro LM, Diaz Berenstein L, Spray TL, Gaynor JW, Fuller S, Keller MS, Harris MA, Whitehead KK, Clancy R, Elci O, Bethel J, Vossough A, Licht DJ. Relationship of cerebral blood flow to aortic-to-pulmonary collateral/shunt flow in single ventricles. *Heart*. 2015;101:1325–1331. doi: 10.1136/heartjnl-2014-307311.
31. Gäddlin PO, Finnström O, Samuelsson S, Wadsby M, Wang C, Leijon I. Academic achievement, behavioural outcomes, and MRI findings at 15 years of age in very low birthweight children. *Acta Paediatr*. 2008; 84:343–349.
32. Pierrat V, Haouari N, Liska A, Thomas D, Subtil D, Truffert P, Groupe d'Etudes en Epidemiologie Perinatale. Prevalence, causes, and outcome at 2 years of age of newborn encephalopathy: population based study. *Arch Dis Child Fetal Neonatal Ed*. 2005; 90:F257–F261.
33. Limperopoulos C, Bassan H, Gauvreau K, Robertson RL Jr, Sullivan NR, Benson CB, Avery L, Stewart J, Soul JS, Ringer SA, Volpe JJ, duPlessis AJ. Does cerebellar injury in premature infants contribute to the high prevalence of long-term cognitive, learning, and behavioral disability in survivors? *Pediatrics*. 2007;120:584–593. doi: 10.1542/peds.2007-1041.
34. Badr LK, Bookheimer S, Purdy I, Deeb M. Predictors of neurodevelopmental outcome for preterm infants with brain injury: MRI, medical and environmental factors. *Early Hum Dev*. 2009;85:279–284. doi: 10.1016/j.earlhumdev.2008.11.005.
35. Cheng HH, Wypij D, Laussen PC, Bellinger DC, Stopp CD, Soul JS, Newburger JW, Kussman BD. Cerebral blood flow velocity and neurodevelopmental outcome in infants undergoing surgery for congenital heart disease. *Ann Thorac Surg*. 2014;98:125–132. doi: 10.1016/j.athoracsur.2014.03.035.
36. Hunt RW, Evans N, Rieger I, Kluckow M. Low superior vena cava flow and neurodevelopment at 3 years in very preterm infants. *J Pediatr*. 2004;145:588–592. doi: 10.1016/j.jpeds.2004.06.056.
37. Eixarch E, Meler E, Iraola A, Illa M, Crispi F, Hernandez-Andrade E, Gratacos E, Figueras F. Neurodevelopmental outcome in 2-year-old infants who were small-for-gestational age term fetuses with cerebral blood flow redistribution. *Ultrasound Obstet Gynecol*. 2008;32:894–899. doi: 10.1002/uog.6249.
38. Leppänen M, Ekholm E, Palo P, Maunu J, Munck P, Parkkola R, Matomäki J, Lapinleimu H, Haataja L, Lehtonen L, Rautava P; PIPARI Study Group. Abnormal antenatal Doppler velocimetry and cognitive outcome in very-low-birth-weight infants at 2 years of age. *Ultrasound Obstet Gynecol*. 2010;36:178–185. doi: 10.1002/uog.7694.
39. Butler RW, Dickinson WA, Katholi C, Halsey JH Jr. The comparative effects of organic brain disease on cerebral blood flow and measured intelligence. *Ann Neurol*. 1983;13:155–159. doi: 10.1002/ana.410130208.
40. Lou HC, Skov H, Henriksen L. Intellectual impairment with regional cerebral dysfunction after low neonatal cerebral blood flow. *Acta Paediatr Scand Suppl*. 1989;360:72–82.
41. Bakker MJ, Hofmann J, Churches OF, Badcock NA, Kohler M, Keage HA. Cerebrovascular function and cognition in childhood: a systematic review of transcranial Doppler studies. *BMC Neurol*. 2014;14:43. doi: 10.1186/1471-2377-14-43.
42. Koide H, Kobayashi S, Kitani M, Tsunematsu T, Nakazawa Y. Improvement of cerebral blood flow and cognitive function following pacemaker implantation in patients with bradycardia. *Gerontology*. 1994;40:279–285.

Neurological Injury and Cerebral Blood Flow in Single Ventricles Throughout Staged Surgical Reconstruction

Mark A. Fogel, Christine Li, Okan U. Elci, Tom Pawlowski, Peter J. Schwab, Felice Wilson, Susan C. Nicolson, Lisa M. Montenegro, Laura Diaz, Thomas L. Spray, J. William Gaynor, Stephanie Fuller, Christopher Mascio, Marc S. Keller, Matthew A. Harris, Kevin K. Whitehead, Jim Bethel, Arastoo Vossough and Daniel J. Licht

Circulation. 2017;135:671-682; originally published online December 28, 2016;
doi: 10.1161/CIRCULATIONAHA.116.021724
Circulation is published by the American Heart Association, 7272 Greenville Avenue, Dallas, TX 75231

Print ISSN: 0009-7322. Online ISSN: 1524-4539